Miscibility of Amphotericin B−Dipalmitoyl Phosphatidyl Serine Mixed Monolayers Spread on the Air/Water Interface

J. Miñones, Jr.,[†] J. Miñones,*[,†] J. M. Rodríguez-Patino,[‡] O. Conde,[†] and E. Iribarnegaray[†]

Departament of Physical Chemistry, Faculty of Pharmacy, University of Santiago de Compostela, Spain, and Department of Chemical Engineering, Faculty of Chemistry, University of Seville, Spain

Received: March 15, 2002; In Final Form: September 18, 2002

Amphotericin B (AmB) monolayers exhibit a phase transition at a surface pressure of 10 mN/m, indicated by a plateau in the $\pi-A$ curves, which is attributed to the reorientation of the AmB molecules from a horizontal to a vertical position. In mixed films with dipalmitoyl phosphatidyl serine (DPPS), this plateau appears at a higher surface pressure, 20 mN/m, independently of the mixed monolayer composition. It is suggested that the presence of the phospholipid in the mixture hinders the reorientation of AmB molecules as a consequence of the formation of a 2:1 AmB/DPPS complex. With the aid of phase diagrams and by application of the Crisp phase rule, the miscibility of the mixed films' components is discussed. To study the monolayers' behavior in the collapse region, subphases of high ionic strength (3 M aq. NaCl) were used. Under these conditions, the existence of two independent collapses was observed; the first corresponds to the ejection of the AmB molecules from the surface, and another is related to the expulsion of the phospholipid. Both components were separated from the 2:1 AmB/DPPS complexes when the monolayer was compressed above 20 mN/m.

Introduction

In the past 20 years, an extraordinary increase in the number of systemic fungal infections has been observed due principally to AIDS patients.[1,2] The problem has recently worsened due to the appearance of multidrug-resistant fungal strains with negative impact on the effectiveness of available antimycotic drugs.[3,4]

The ideal antifungal agent should be characterized by the following: high antifungal activity, broad antimycotic spectrum, fungicidal action (important for immune-suppressed patients), low host toxicity, reluctance to induce specific resistance, and the ability to overcome multidrug resistance. Unfortunately, none of the currently available clinical antimycotics fulfill all of the above-mentioned requirements. Therefore, perhaps the most promising compound is still the polyene antibiotic amphotericin B (AmB) called the "golden standard" among antimycotics. AmB is an amphiphilic molecule containing an apolar side formed by seven conjugated double bonds and a polar side with seven hydroxyl groups and an ester carbonyl group. A mycosamine residue is attached to one end, providing a free amino group (Scheme 1). This compound has been clinically used for over 40 years. It exhibits the broadest spectrum of activity among clinically useful antifungals, and its fungicidal action makes AmB almost irreplaceable in the treatment of infections in immune-suppressed patients. It also exhibits a unique property among the clinical antifungals of being reluctant to induce resistance and it is able to overcome multidrug resistance. However, it is highly toxic to the host, capable of causing severe complications such as renal damage and hemolysis.[1] This is due to the fact that the mechanism of action of AmB on fungi cells, which contain ergosterol, is similar to its mechanism of action on mammalian cells, which are formed by cholesterol. AmB

SCHEME 1

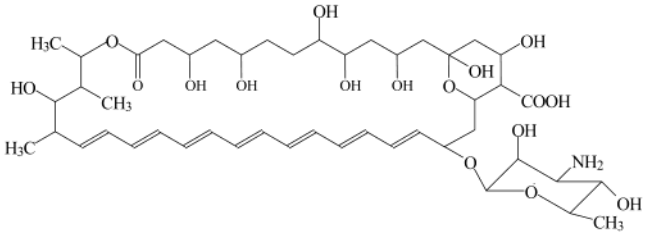

interacts with both sterols and forms transmembrane channels through which free diffusion of many components essential for cell life occurs, leading to cell death.[6,7] Its insolubility in water also constitutes an additional serious problem.

Several formulations, such as liposomal preparations, have been developed to reduce the toxicity of AmB and improve its water solubility.[8] Different studies have demonstrated that AmB administered in this form is much less toxic to the host, without loss of its antifungal potency.[9−15] The reasons why AmB is less toxic in liposomes than in the free form (fungizone) are not precisely known, even though there seems to exist a certain relationship between the liposomal composition and the toxicity of the drug, given that AmB-containing liposomes composed of phospholipids with saturated acyl chains are nontoxic, whereas AmB liposomes composed of phospholipids containing unsaturated acyl chains are almost as toxic as AmB itself.[13]

These results allow one to suppose that there exists a certain affinity between the drug and the vehicle-forming phospholipids. Lance et al.[16] have shown the existence of significant interactions between AmB and saturated phospholipids in monolayers. In our recent studies[17−19] we have postulated the formation of a stable AmB/phospholipid complex when the molar proportion of these components is 2:1. In this work, the formation of a complex of the same stoichiometry for the anionic phospholipid DPPS is supported, and the miscibility of the AmB−DPPS

* Corresponding author.
[†] University of Santiago de Compostela.
[‡] University of Seville.

10.1021/jp0207275 CCC: $25.00
Published on Web 04/04/2003

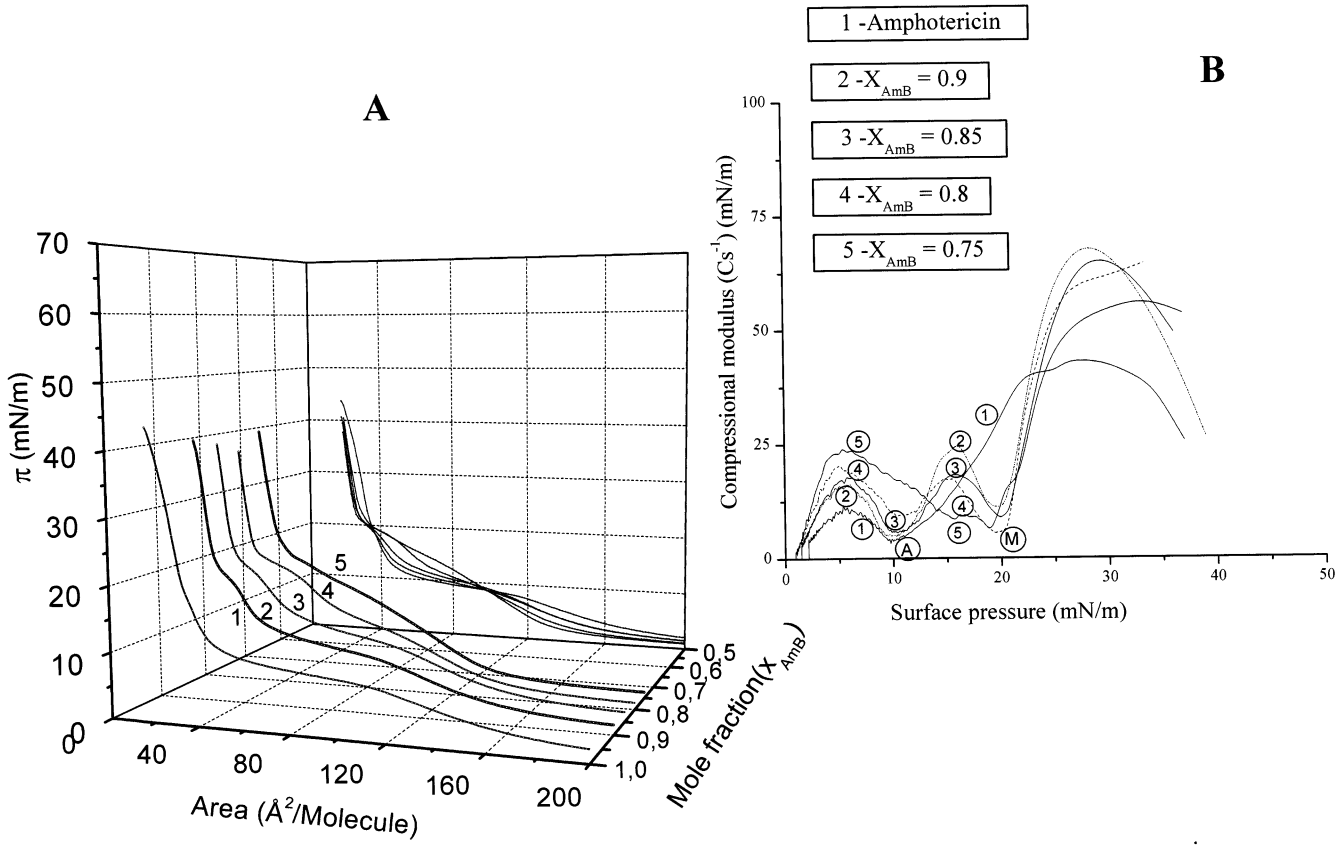

Figure 1. $\pi-A$ isotherms for AmB−DPPS mixed monolayers ($X_{AmB} > 0.7$) spread on water at 20° C. X_{AmB} = mole fraction of amphotericin B. Inset: compressional modulus−surface pressure ($C_s^{-1}-\pi$) plots.

system's components as a function of their composition is investigated. The research was carried out using a classic surface balance for the measurements of surface pressure together with a more advanced technique—Brewster angle microscopy (BAM)—for the observation of the monolayer's topography.

Material and Methods

DL-α-Phosphatidyl-L-serine dipalmitoyl (98% purity) was purchased from the Sigma Chemical Company. Squibb (Bristol-Myers Lab) supplied AmB, and its purity was specified as higher than 95%. Both were used as received. DPPS was dissolved in a 4:1 (v:v) mixture of chloroform (p.a. Merck) and absolute ethanol (p.a. Merck). AmB was dissolved in a 3:1 (v:v) mixture of dimethylformamide and 1 M aq HCl. Mixed solutions of different mole fractions (X_{AmB}) of AmB−DPPS were prepared by mixing certain volumes of AmB and DPPS stock solutions. Aliquots of approximately 200 μL (4.25×10^{16} molecules) of the mixed solutions were then spread onto the water surface by means of a micrometric syringe. The solvent was allowed to evaporate for about 10 min before monolayer compression. Pure water (resistivity 18 MΩ. cm) was provided by a Milli-Q system coupled to a Milli-RO reverse osmosis unit (Millipore Co.). The purity of the subphase surface was controlled during compression by surface tension measurements of an uncovered subphase. In all cases, the surface pressure obtained in these blank tests was less than 0.1 mN/m (i.e., of the order of experimental accuracy). When required, NaCl (p.a. Merck) was added to the water subphase to obtain a 3 M substrate.

Isotherms of mixed drug−phospholipid Langmuir monolayers at several drug/phospholipid ratios were carried out with a KSV 5000 Langmuir trough equipped with a Wilhelmy plate as surface pressure sensor (accuracy of 0.1 mN/m). The surface pressure versus area per molecule ($\pi-A$) isotherms were registered on symmetrical compression of the monolayers with two barriers at a constant speed of 30 mm/min (8.5 Å^2 molecule^{-1} min^{-1}). The experiments were performed at 20 ± 1° C and the isotherms represent the average of at least four measurements for each drug composition.

A BAM 2 Brewster angle microscope from NFT (Göttingen, Germany), equipped with a 30 mW laser emitting p-polarized light at 690 nm wavelength, allowed the imaging of the surface with a resolution of 2 μm. The reflected light at the Brewster angle (53.1°) was detected by means of a CCD camera and recorded with image processing software in order to further improve the brightness on videotape and contrast of the images. Relative reflectivity (I) measurements were performed during monolayer compression−expansion cycles using different shutter speeds (within the range of 1/50 to 1/500 s).[20]

Results and Discussion

Figure 1 shows the $\pi-A$ isotherms obtained for pure AmB and AmB/DPPC mixtures of compositions ranging from $X_{AmB} = 0.75$ to $X_{AmB} = 0.9$ spread on water (pH = 6). The curve for pure AmB exhibits three regions of different slope. The first, at low surface pressures, corresponds to a liquid expanded state with a compressional modulus ($C_s^{-1} = -A\, d\pi/dA$) relatively low ($C_s^{-1} = 14$ mN/m at 5 mN/m). At $\pi = 10$ mN/m, the monolayer undergoes a phase transition, and, as a consequence, a plateau in the $\pi-A$ isotherm is observed. Beyond this transition region, the pronounced slope of the isotherm reveals that the monolayer is in a liquid condensed state. Thus, the molecular packing increases with the film compression, but without collapsing, due to the instability of the monolayer that results from its dissolution into the aqueous subphase.[21,22]

TABLE 1: Values of Limiting Areas (A_0) and Surface Pressures of Phase Transitions (π_t) Corresponding to Pure Monolayers and Mixed Films of AmB−DPPS Spread on Water at 20 °C[a]

X_{AmB}	$A_{0(exp.)}$ (Å²/molecule)	$A_{0(cond.)}$ (Å²/molecule)	π_t (mN/m)	
			M	*A*
DPPS	58.2	55.3		
0.1	69.4	46.7	19.4	
0.3	101.7	44.2	19.3	
0.5	134.2	41.7	18.9	
0.7	143.2	33.6	19.4	
0.75	138.0	37.8	18.9	
0.8	152.9	33.9	19.5	11.0
0.85	170.2	34.5	19.9	10.5
0.9	173.0	35.0	19.5	9.9
AmB	169.6	44.4		9.9

[a] $A_{0(exp.)}$ and $A_{0(cond.)}$ denote the limiting areas at the expanded and condensed states, respectively.

The first-order phase transition of AmB monolayer at $\pi \sim 10$ mN/m has been attributed by Saint Pierre Chazalet et al.[23] to the progressive change in the orientation of the AmB molecules from the horizontal to a vertical position. In the latter case the molecular area is about 55 Å²/molecule (a value corresponding to the end of the plateau), which coincides with that obtained by using molecular models[23] for the molecule in a vertical position. This value decreases upon further compression to 25 Å²/molecule, as a consequence of the desorption from the surface of vertically oriented molecules.[24]

Our recent BAM studies[25] confirmed the change in orientation of the AmB molecules given that the increase in the relative reflectivity of the film produced during the compression, from the expanded to the condensed state, corresponds to a 3-fold increase in the film thickness. This increase is close to the value calculated when the AmB molecule changes from the horizontal to the vertical position.[23,26,27]

AmB−DPPS mixed films (for X_{AmB} ranging from 0.9 to 0.8) exhibit a phase transition similar to that observed for pure AmB, which appears as a pseudo-plateau in the $\pi-A$ isotherms (Figure 1, curves 2−4). The surface pressure relative to this transition increases slightly as the proportion of AmB in the mixed monolayer decreases (Table 1). On the other hand, the length of the corresponding pseudo-plateau in the $\pi-A$ curves diminishes as the proportion of DPPS in the mixed film increases, and finally when $X_{AmB} = 0.75$, it disappears (Figure 1, curve 5).

These phase transitions are clearer in the plots of the compressional modulus (C_s^{-1}) as a function of the surface pressure (inset of Figure 1), wherein the minimum values (*A*) of C_s^{-1} correspond to the above-mentioned phase transitions. These values appear at slightly higher surface pressures as the proportion of the phospholipid in the mixed monolayer increases, becoming less significant until it disappears when $X_{AmB} = 0.75$.

Another phase transition, characterized by the existence of a small plateau in the $\pi-A$ curves and by a minimum *M* in the $C_s^{-1}-\pi$ plots, was observed in these mixed monolayers at surface pressures around 19−20 mN/m. Although the surface pressure corresponding to this second plateau hardly changes with the composition of the mixed films (Table 1), its length and its flatness (determined by the values of C_s^{-1}, given that the smaller these are, the flatter the plateau) increase as the proportion of DPPS in the monolayer increases (inset of Figure 1). This phenomenon is observed more clearly in the mixtures with $X_{AmB} < 0.75$ (Figure 2), even though in this case the length and the flatness of the plateau increase in a manner opposite to that indicated above. That is, the greater the proportion of DPPS, the smaller the values of these parameters (inset, Figure 2). Nevertheless, the surface pressure corresponding to the plateau remains constant, around 19−20 mN/m (Table 1).

In summary, it can be concluded that the progressive addition of DPPS to the AmB monolayer causes the disappearance of the phase transition *A* (at $\pi \approx 10$ mN/m), typical of the polyene, provoking the appearance of a new phase transition *M* at a higher surface pressure (at $\pi \approx 20$ mN/m). The length and flatness of the plateau in the $\pi-A$ curves, corresponding to this new transition *M*, increase as the proportion of AmB increases in mixed films with a composition $X_{AmB} < 0.7$, and decreases when $X_{AmB} > 0.7$. Consequently, the higher values of these parameters correspond to the mixture of $X_{AmB} = 0.7$, in which case the proportion of the components in the mixed film is 2.33:1 (AmB/DPPS), that is to say, approximately 2:1 ($X_{AmB} = 0.66$).

The application of Brewster angle microscopy to this mixture confirms the existence of a phase transition at $\pi \approx 20$ mN/m, as is demonstrated by the fact that the relative reflectivity curve (*I*), as a function of the surface pressure (π), shows a significant discontinuity at this surface pressure (Figure 3, curve *M*). The $I-\pi$ curve shows a considerable number of reflectivity peaks of noticeable intensity, which are attributed to AmB domains, seen as a white mass in the BAM images (Figure 4A). As the compression progresses, the domains become more densely packed together to form compact structures (Figure 4B,C), with inverted images as the analyzer rotated 60° with respect to the plane of incidence (image C'). The optical anisotropy disappears when the reflectivity becomes constant, resulting in a BAM image that is practically uniform (Figure 4D). In summary, the existence of optical anisotropy through the phase transition at 20 mN/m shows no bilayer or multilayer formation in this transition region. In light of these results and given that at the Brewster angle, *I* is proportional to ϵ^2 (where ϵ is the film thickness),[28] the increase of *I* (or ϵ) in Figure 3 can be attributed to the change in the orientation of the AmB molecules from their initial horizontal position, to a more vertical position, even though such reorientation is hindered by the existence of interactions between AmB and DPPS molecules. For this reason, the transition occurs at a higher surface pressure (20 mN/m), instead of at 10 mN/m as for a pure AmB monolayer (AmB curve of Figure 3). Furthermore, the absence of reflectivity peaks, as well as the existence of constant relative reflectivity values for the DPPS monolayer, indicates that the tilt of the apolar chains does not change throughout compression. This fact reinforces the hypothesis that the change in the reflectivity (or thickness) of the mixed films is due solely to the AmB.

For the mixed film with $X_{AmB} = 0.9$, the $I-\pi$ curve coincides with that of AmB in the surface pressure range between 0 and 13 mN/m (Figure 5A, curves *M* and AmB, respectively). Even then, the intensity of the reflectivity peaks is nearly the same in both cases. At surface pressures higher than 13 mN/m, both curves differ, the *I* values of the *M* curve remaining nearly unalterable, whereas those of the AmB curve continue to increase. At surface pressures around 20 mN/m, the reflectivity of *M* abruptly increases. These results confirm those of Figure 1 (curve 2) since the existence of two plateaus in the $\pi-A$ curves corresponds to the presence of two discontinuities in the I−π diagrams. The BAM pictures relative to these plateaus (Figure 5, images B and C) show the existence of large AmB domains, which mask the presence of the phospholipid in the mixed monolayer even at low surface pressures. Accordingly, the BAM images obtained do not provide noticeable information about the monolayer texture in these phase transitions.

The results of Figure 6, corresponding to the AmB−DPPS

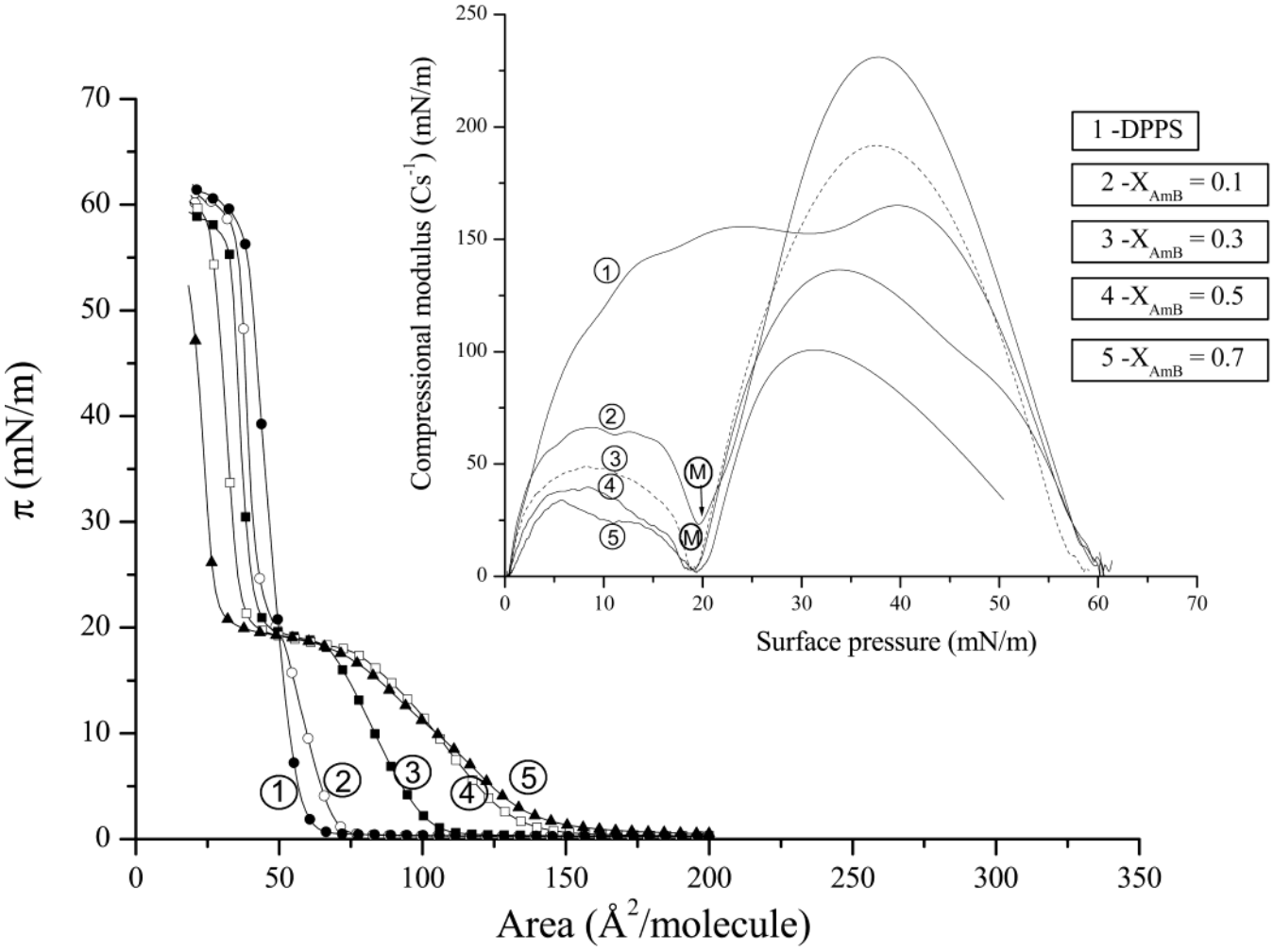

Figure 2. $\pi-A$ isotherms for AmB−DPPS mixed monolayers ($X_{AmB} < 0.75$) spread on water at 20° C. X_{AmB} = mole fraction of amphotericin B. Inset: compressional modulus−surface pressure ($C_s^{-1}-\pi$) plots.

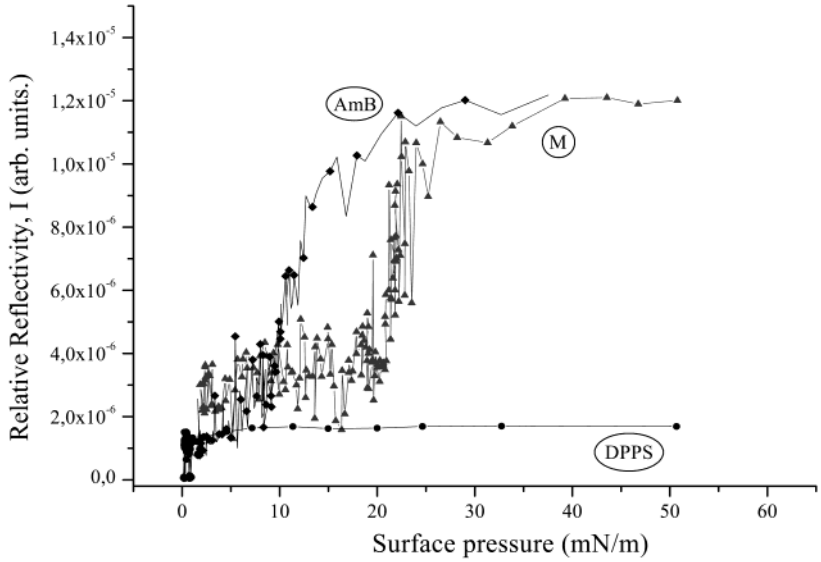

Figure 3. Relative reflectivity (I)−surface pressure (π) curves corresponding to the compression of AmB, DPPS, and the AmB−DPPS mixture with $X_{AmB} = 0.7$ spread on water at 20 °C.

mixture with $X_{AmB} = 0.9$ compressed at different waiting times after its spreading on the interface, confirm that the existence of interactions between the mixed film components is a dynamic process. In fact, when the mixed film is compressed after a 10 min waiting time, the isotherm obtained (curve 1) exhibits the two plateaus mentioned in Figure 1, where the first (at 10 mN/m) corresponds to the reorientation of the free excess AmB molecules (with respect to the 2:1 AmB/DPPS complex), and the second (at 20 mN/m) is attributed to the change in orientation of the AmB molecules which are embedded in the complex with

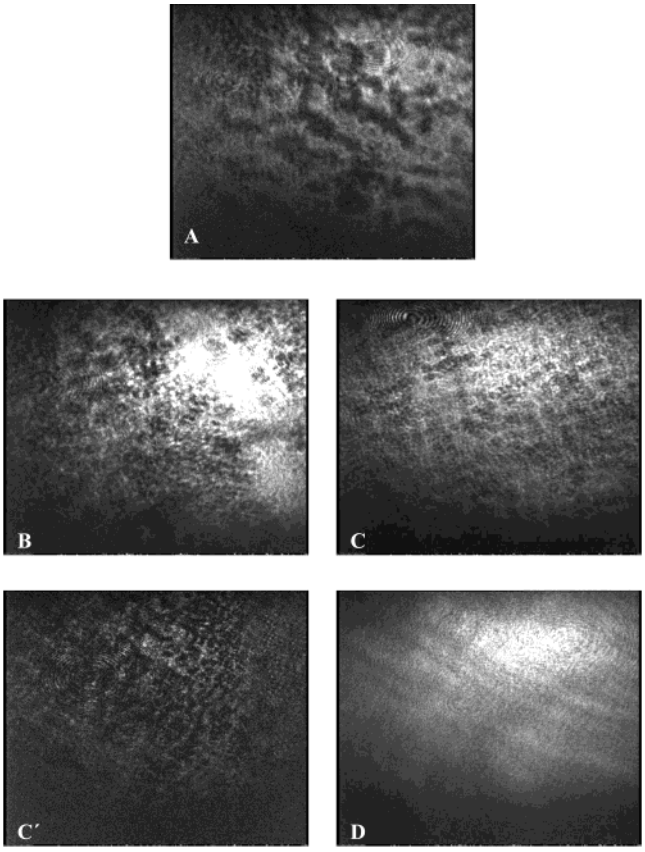

Figure 4. BAM images corresponding to the mixture of AmB and DPPS with $X_{AmB} = 0.7$. (A): AmB domains at 0.4 mN/m (shutter speed 1/50 s.). (B): increase of AmB domain density at 9.1 mN/m (shutter speed 1/125 s.). (C) and (C′): AmB domains with optical anisotropy at 19.5 mN/m (C′, analyzer at 60°). (D): Image of high intensity without optical anisotropy (shutter speed 1/500 s.).

the phospholipid. As the waiting time between the spreading of the film and the beginning of compression is increased, the length of the first plateau decreases (which is accompanied by a small increase in the transition surface pressure), and, on the other hand, the second plateau becomes longer (without surface pressure modification) (curves 2 and 3). At last, when the waiting period is sufficiently long, the first plateau disappears completely, and the second acquires an appreciable length and flatness (curve 4). Since AmB is desorbed slowly, the disappearance of the first plateau is provoked, in part, by the dissolution of the free polyene molecules in the subphase, and also by the progressive interaction with the phospholipid, which accounts for the increase of the surface pressure necessary for the reorientation of the AmB molecules and the growth of the second plateau. In accordance with this, the greater the length of this plateau, the more important the interactions between the mixture's components. Thus, the strongest interaction seems to occur when the film components are in the 2:1 proportion (AmB/DPPS), because the plateau in the $\pi-A$ isotherm corresponding to the mixed monolayer of this composition ($X_{AmB} \approx 0.7$) exhibits the maximum length and flatness (Figure 2). In consequence, we postulate that in this mixture the film components form a stable complex of stoichiometry 2:1, responsible for the monolayer phase transition at 20 mN/m.

Using the phase diagram of Figure 7, and by application of Crisp's phase rule [29,30] in the form: $P = C - F + 1$ to the *A* and *M* transitions, the miscibility of the film-forming components in the mixed systems can be determined. In the mixtures with excess AmB ($X_{AmB} > 0.66$), as compared to the mixture

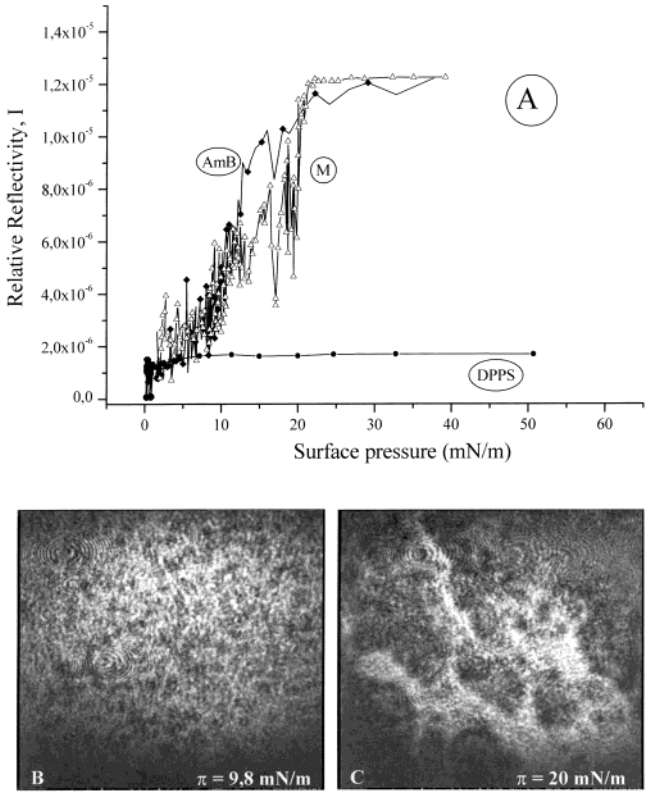

Figure 5. (A) Relative reflectivity−surface pressure curves corresponding to the compression of AmB, DPPS, and AmB−DPPS ($X_{amB} = 0.9$) monolayers spread on water. (B) and (C) BAM images corresponding to the phase transitions of AmB−DPPS ($X_{amB} = 0.9$) mixed film at 9.8 mN/m and 20 mN/m, respectively.

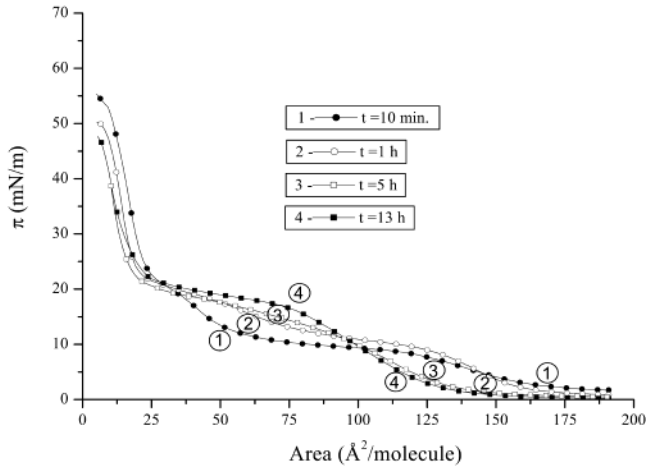

Figure 6. Time dependence of the compression isotherms for AmB−DPPS mixed monolayers of composition $X_{AmB} = 0.9$.

for the 2:1 complex formation, two phases (P) in equilibrium coexist along the *A* line. Indeed, in this case, the number of components, *C*, is 2 (AmB and DPPS), and given that the transition pressure varies with the composition, the degrees of freedom (*F*) are 1, and therefore, $P = 2$. Consequently, at surface pressures below 10 mN/m ($\pi < \pi_A$), the homogeneous monolayers consist of AmB/DPPS complexes (C) mixed with the excess of free AmB molecules (AmB_h), horizontally oriented. The same occurs at surface pressures above 10 mN/m ($\pi > \pi_A$), even though in this case the excess AmB molecules are found vertically oriented (AmB_v) as a consequence of the change in orientation that they experience along the transition *A*.

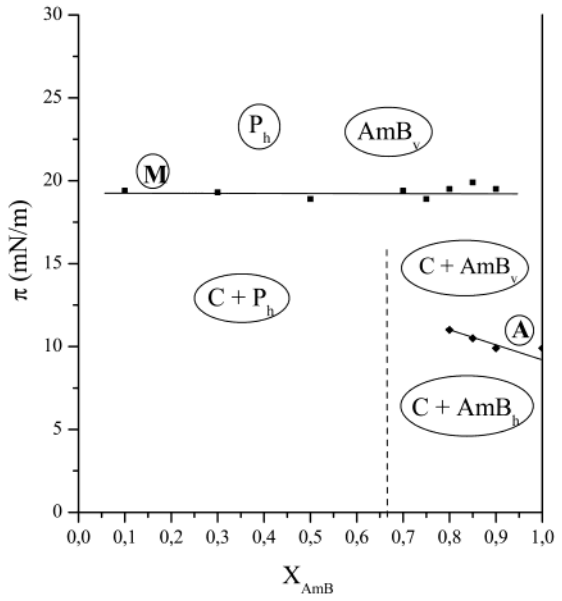

Figure 7. Phase diagram for AmB−DPPS mixed monolayers spread on water at 20 °C. C denotes the AmB/DPPS complex of stoichiometry 2:1. AmB_h denotes horizontally oriented AmB molecules. AmB_v corresponds to amphotericin B molecules oriented vertically. Ph corresponds to phospholipid (DPPS) monolayer.

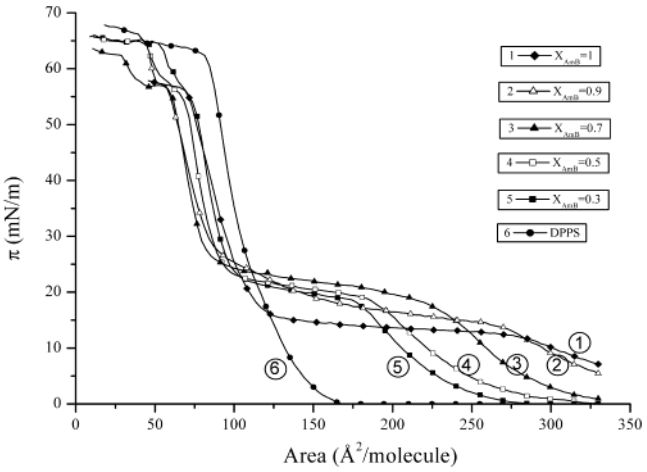

Figure 8. $\pi-A$ curves for AmB−DPPS mixed monolayers spread on 3 M aq NaCl subphases at 20 °C.

Throughout the *M* transition, the surface pressure practically does not vary with the monolayer composition (Table 1). In this situation, the system is invariable ($F = 0$) and therefore $P = 3$. This means that the reorientation of the AmB molecules that form part of the complex (at 20 mN/m) provokes its segregation, originating two immiscible phases: that formed by the AmB molecules (orientated vertically), and the other one constituted by the phospholipid (P_h). The same occurs in the mixtures containing phospholipid in excess ($X_{AmB} < 0.66$). In these cases, the homogeneous phase at surface pressures below that of the transition M is composed of C complexes mixed with an excess of phospholipid (P_h) molecules.

The behavior of the mixed films in the collapse region allows us to confirm the immiscibility of the film-forming components after the complex break-up. Since it is difficult to determine precisely the collapse pressure of the AmB monolayer on water, due to its solubility, high ionic strength substrates (3 M aq NaCl) were used for this purpose (Figure 8). The mixtures of different composition exhibit an inflection (or pseudo-plateau) at a surface pressure around 55 mN/m, which coincides with the collapse

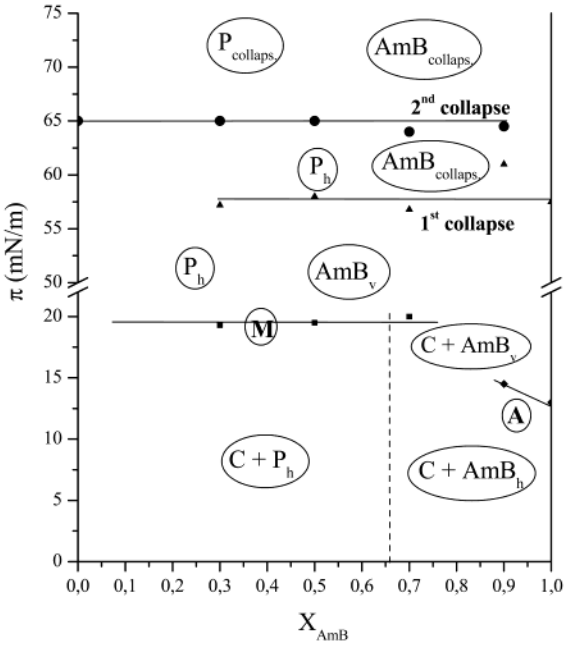

Figure 9. Phase diagram for AmB−DPPS mixed monolayers spread on 3 M aq NaCl subphase (see further information in the text).

pressure for the pure AmB monolayer. Furthermore, for all investigated mixtures, a second collapse is observed at approximately the same surface pressure as that for the pure phospholipid monolayer (65 mN/m). This behavior is typical of monolayers formed by immiscible components.[29,30] The phase diagram corresponding to these mixtures is shown in Figure 9. The application of the phase rule at the first collapse leads to the existence of three phases in equilibrium ($P = 3$), given that at these conditions $C = 2$ and $F = 0$ (the collapse pressure is independent of the composition of the system). Therefore, at the collapse point there are three surface phases in equilibrium: (i) that formed by phospholipid (P_h) molecules segregated from the complex, (ii) that composed of AmB molecules vertically oriented (AmB_v) and also segregated from the complex, and (iii) the 3-D phase formed by the collapsed AmB ($AmB_{collapse}$).

The second plateau, observed at surface pressures around 65 mN/m, corresponds to the collapse of the phospholipid molecules. In this situation there are also three phases in equilibrium: the two 3-D phases formed by the collapsed AmB ($AmB_{collapse}$) and by the collapsed phospholipid ($P_{collapse}$), and the surface phase constituted by uncollapsed phospholipid molecules (P_h) segregated from the complex.

Acknowledgment. This work was supported by Project PGIDT99PXI20302B (Xunta de Galicia).

References and Notes

(1) Georgopapadakou, N. H. *Curr. Opin. Microbiol.* **1994**, *1*, 547.
(2) de Pauw, B. E.; Meunier, F. *Chemotherapy* **1999**, *45* (suppl. 1), 1.
(3) Vanden Bosche, H.; Warnock, D. W.; Dupont, B.; Kerrdge, D.; Sen Gupta, S.; Improvisi, L.; Marichal, P.; Odds, F. C.; Provost, F.; Ronin, O. *J. Med. Vet. Mycol.* **1994**, *32*, (suppl. 1), 189.
(4) Wong-Beringer, A.; Jacobs, R. A.; Guglielmo, B. *J. Clin. Infect. Dis.* **1998**, *27*, 603.
(5) Carlson, M. A.; Condon, R. E. *J. Am. Coll. Surg.* **1994**, *179*, 361.
(6) Bolard, J. *Biochim. Biophys. Acta* **1986**, *864*, 257.
(7) Brajtburg, J.; Bolard, J. *Clin. Microbiol. Rev.* **1996**, *9*, 512.
(8) López-Berestein, G. In *Liposomes in therapy of infectious diseases and cancer*; López-Berestein, G., Fidler, J. J., Eds.; Alan R. Liss. Inc.: New York, 1989; pp 317−327.

(9) New, R. R. C.; Chance, M. L.; Health, S. *J. Antimicrob. Chemother.* **1981**, *8*, 371.

(10) Taylor, R. L.; Willians, D. M.; Craven, P. C.; Graybill, J. R.; Drutz, D. J.; Magee, W. E. *Am. Rev. Respir. Dis.* **1982**, *125*, 610.

(11) Graybill, J. R.; Craven, P. C.; Taylor, R. L.; Willians, D. M.; Magee, W. E. *J. Infect. Dis.* **1982**, *145*, 748.

(12) López-Berestein, G.; Mehta, R.; Hopfer, R. L.; Mills, K.; Kasi, L.; Mehta, K.; Fainstein, V.; Luna, M.; Hersh, E. M.; Juliano, R. *J. Infect. Dis.* **1983**, *143*, 939.

(13) Juliano, R. L.; Grant, C. W. M.; Barber, K. R.; Kalp, M. A. *Mol. Pharmacol.* **1987**, *31*, 1.

(14) López-Berestein, G.; Bodey, G. P.; Frankel, L. S.; Mehta, K. *J. Clin. Oncol.* **1987**, *5*, 310.

(15) Sculier, J. P.; Coune, A.; Meunier, F.; Brassinne, C.; Laduron, C.; Hollaert, C.; Collette, N.; Heymans, C.; Klastersky, J. *Eur. J. Cancer Clin. Oncol.* **1988**, *24*, 527.

(16) Lance, M. R.; Washington, C.; Davis, S. S. *Pharm. Res.* **1996**, *13*, 1008.

(17) Miñones, J., Jr.; Miñones, J.; Conde, O.; Seoane, R.; Dynarowicz-Latka, P. *Langmuir* **2000**, *16*, 5743.

(18) Miñones, J., Jr.; Miñones, J.; Conde, O.; Rodriguez-Patino, J. M.; Dynarowicz-Latka, P. *Langmuir* **2002**, *18*, 2817.

(19) Miñones, J., Jr.; Conde, O.; Miñones, J.; Rodriguez-Patino, J. M.; Seoane, R. *Langmuir* (in press).

(20) Rodriguez-Patino, J. M.; Carrera Sánchez, C.; Rodriguez Niño, M. R. *Langmuir* **1999**, *15*, 2484.

(21) Rey Gómez-Serranillos, I.; Miñones, J., Jr.; Seoane, R.; Conde, O.; Casas, M. *Prog. Colloid Polym. Sci.* **1738**, *16*, 5743.

(22) Rey Gómez-Serranillos, I.; Dynarowicz-Latka, P.; Miñones, J., Jr.; Seoane, R. *J. Colloid Interface Sci.* **2001**, *234*, 351.

(23) Saint-Pierre-Chazalet, M.; Thomas, C.; Dupeyrat, M.; Gary-Bobo, C. M. *Biochim. Biophys. Acta* **1988**, *944*, 477.

(24) Seoane, J. R.; Vila Romeu, N.; Miñones, J.; Conde, O.; Dynarowicz, P; Casas, M. *Prog. Colloid Polym. Sci.* **1997**, *105*, 173.

(25) Miñones, J., Jr.; Carrera, C.; Dynarowicz-Latka, P.; Miñones, J.; Conde, O.; Seoane, R.; Rodriguez-Patino, J. M. *Langmuir* **2001**, *17*, 1477.

(26) Wójtowicz, K.; Gruszecki, W. I.; Walicka, M.; Barwicz, J. *Biochim. Biophys. Acta* **1998**, *1373*, 220.

(27) Van Hoogevest, P.; de Kruiff, B. *Biochim. Biophys. Acta* **1978**, *511*, 397.

(28) Azzam, R. M. A.; Bashara, N. M. In *Ellypsometry and Polarized light*, 1st ed.; North-Holland: Amsterdam, 1997.

(29) Crisp, D. J. In *Surface Chemistry (Supplement to Research);* Butterworth: London, 1949; pp 17−35.

(30) Gaines G., Jr. In *Insoluble Monolayers at Liquid−Gas Interface*; Prigogine, I., Ed.; Interscience: New York, 1966; p 289.